

Supplementary Materials for “High T_c superconductivity in Heavy Rare Earth hydrides”

Hao Song(宋昊)¹, Zihan Zhang(张子涵)¹, Tian Cui(崔田)^{2,1,*}, Chris J. Pickard^{3,4}, Vladimir Z. Kresin⁵, Defang Duan(段德芳)^{1,†}

¹*State Key Laboratory of Superhard Materials, College of Physics, Jilin University, Changchun 130012, China*

²*Institute of High Pressure Physics, School of Physical Science and Technology, Ningbo University, Ningbo 315211, China*

³*Department of Materials Science & Metallurgy, University of Cambridge, 27 Charles Babbage Road, Cambridge CB3 0FS, United Kingdom*

⁴*Advanced Institute for Materials Research, Tohoku University 2-1-1 Katahira, Aoba, Sendai, 980-8577, Japan*

⁵*Lawrence Berkeley Laboratory, University of California at Berkeley, Berkeley, CA 94720, USA*

Corresponding authors email: *cuitian@nbu.edu.cn

Corresponding authors email: †duandf@jlu.edu.cn

Content

1. Computational method	S2
2. The reliability of DFT calculations	S3
3. Convex hull diagram of Yb-H	S4
4. Structural parameters, enthalpy difference curves and phonon dispersion of Yb-H	S5
5. Electronic properties of YbH ₆	S9
6. Convex hull diagram of Lu-H and Tm-H	S10
7. Equations for calculating T_c and related parameters	S12
8. Superconductive properties	S16
References	S22

1. Computational method

For the structure searching we used the *ab initio* random structure searching (AIRSS) approach method^[1,2] and the underlying energetic simulations were performed with the CASTEP code^[3-5]. The ultrasoft pseudopotentials^[6] with the valence electrons Yb ($5s^25p^64f^{14}6s^2$), Tm ($5s^25p^64f^{13}6s^2$), Lu ($5s^25p^64f^{14}5d^16s^2$) and H ($1s^1$), Perdew-Burke-Ernzerhof generalized gradient approximation^[7], a plane-wave cutoff of 400 eV and Monkhorst-Pack meshes^[8] k -point spacing of $2\pi \times 0.07 \text{ \AA}^{-1}$ were used in these searches. Extensive structure searches were performed at 100, 200 and 300 GPa with 1 to 24 hydrogen atoms and 1-4 ytterbium atoms, each structure search at fixed pressure yielded about 7000 structures. Then we re-optimized the structures on the convex hull with high accuracy parameters (a plane-wave cutoff of 700 eV and Monkhorst-Pack meshes k -point spacing of $2\pi \times 0.03 \text{ \AA}^{-1}$ were used) to re-confirm the convex hull. Structure searches for Tm-H and Lu-H system were also performed by AIRSS code. Phonon spectra and electron–phonon coupling (EPC) were studied in the framework of density-functional perturbation theory implemented in the Quantum ESPRESSO package^[9]. Ultrasoft pseudopotentials were used with a kinetic energy cutoff of 80 Ry. We adopted $18 \times 18 \times 18$ k-points grid and $6 \times 6 \times 6$ q-points for $I\bar{m}\bar{3}m$ -YbH₆. The superconducting transition temperatures T_c are evaluated with use of the Eliashberg equation^[10] with a Coulomb pseudopotential $\mu^*=0.1-0.13$. We employed three different methods: the Allen–Dynes-modified McMillan equation (Mc-A-D) with correction factors^[11]; an approach with self-consistent iterations (IA)^[11-13], and the Gor’kov-Kresin theory (G-K)^[14].

2. The reliability of DFT calculations

We first evaluated the equation of state (EOS) for YbH_2 . Then it was compared with the experimental EOS to assess the reliability of our DFT calculations (see Fig. S1). One can see that for the low-pressure phase $Pnma$ of YbH_2 , calculations using the on the fly pseudo-potentials poorly reproduce the experimental EOS; there is a significant volume discrepancy at the same pressure. The ultra-soft pseudo-potentials calculations substantially improve the agreement with the experiment; the agreement is further improved with the DFT+U scheme. One can see that there is a good agreement between the theory and experiment for the high-pressure phase $P6_3/mmc$ of YbH_2 , if we use the ultra-soft pseudo-potentials scheme. The authors of previous work concerned with ytterbium hydrides [15], used a Hubbard $U = 5$ eV for lower pressure phases and $U= 0$ eV for high-pressure phases to reproduce available experimental data, in clear agreement with our results (see Fig. S1).

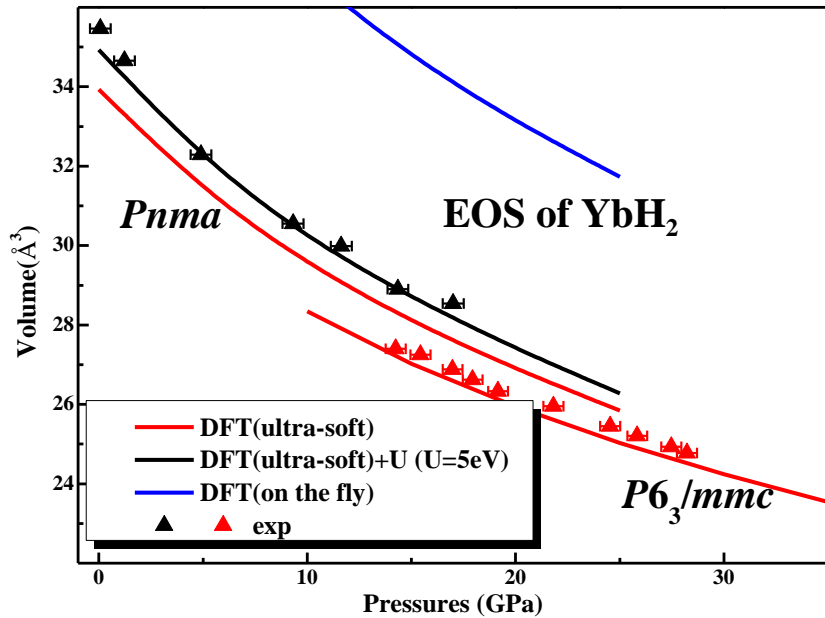


Fig. S1. Volumes as a function of pressures for low pressure phase $Pnma$ and high pressure phase $P6_3/mmc$ for YbH_2 calculated using the DFT with ultra-soft (red line) and on the fly potentials (blue line), DFT with ultra-soft potentials plus Hubbard repulsion (DFT+U, black line), and compared with experiment for YbH_2 [16] (solid triangle).

3. Convex hull diagram of Yb-H

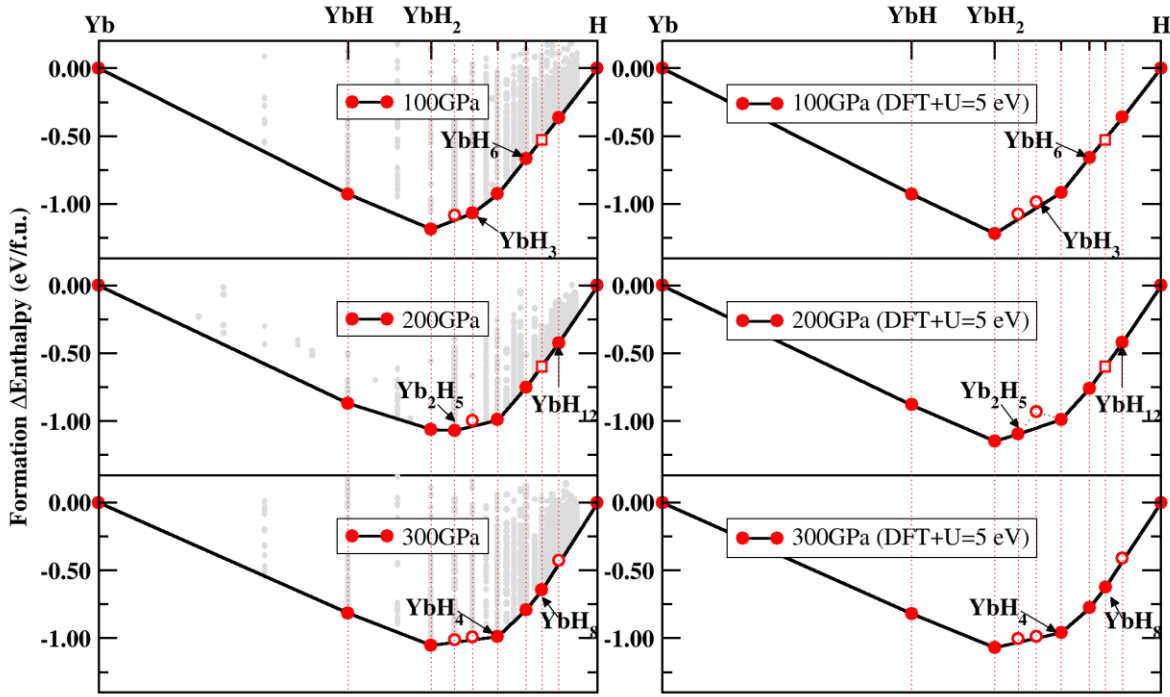


Fig. S2. Convex hull of the Yb-H without and with DFT+U ($U=5$ eV) at 100, 200 and 300 GPa. The solid circle, open circle and open square symbols indicate that the structures are thermodynamic stable, thermodynamic unstable and dynamic unstable, respectively. As can be seen, DFT+U slightly changes the convex-hull. With DFT+U, YbH_3 is off the convex hull at 100 GPa; without DFT+U, YbH_3 is off the convex hull at 200 GPa.

4. Structural parameters, enthalpy difference curves and phonon dispersion of Yb-H

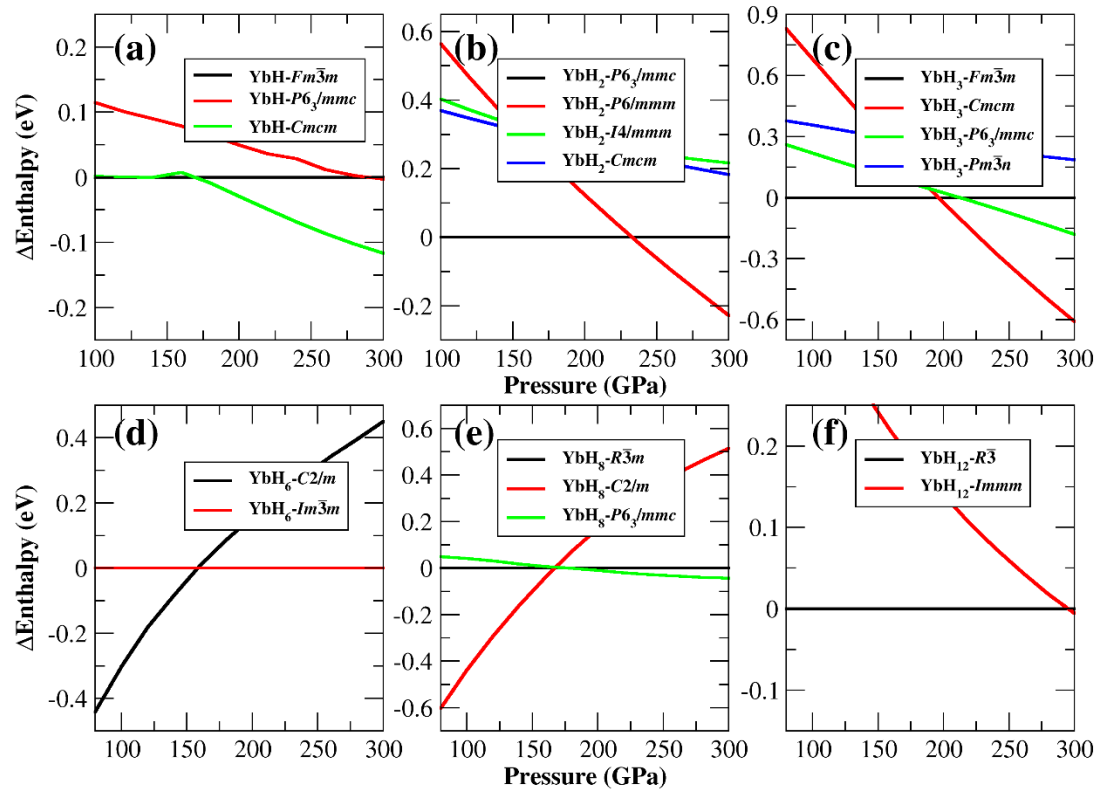


Fig. S3. The enthalpy difference (ΔH) curves of YbH_n ($n=1, 2, 3, 6, 8$ and 12) from 100 to 300 GPa.

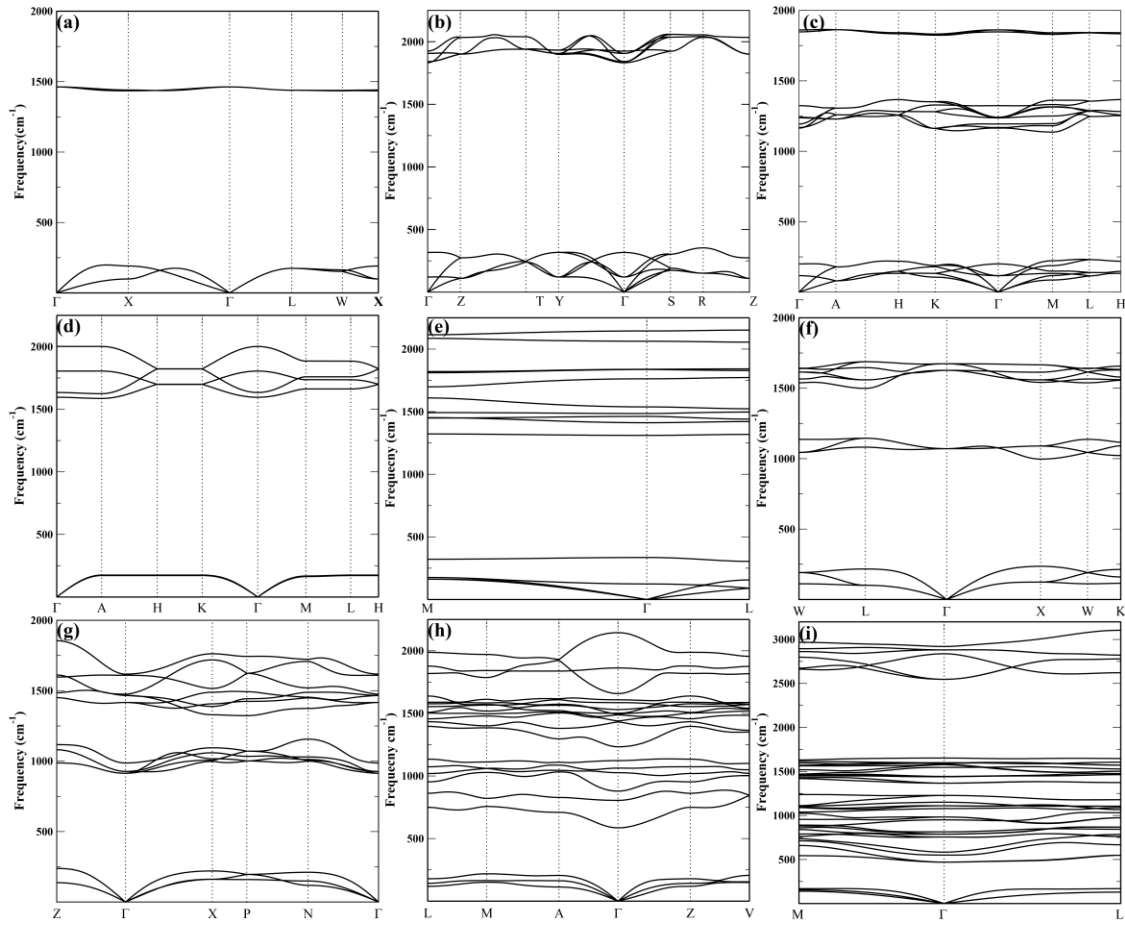


Fig. S4. Phonon dispersion of (a) $Fm\bar{3}m$ -YbH at 100 GPa, (b) $Cmcm$ -YbH at 250 GPa, (c) $P6_3/mmc$ -YbH₂ at 100 GPa, (d) $P6/mmm$ -YbH₂ at 300 GPa, (e) $R\bar{3}m$ -Yb₂H₅ at 200 GPa, (f) $Fm\bar{3}m$ -YbH₃ at 100 GPa, (g) $I4/mmm$ -YbH₄ at 100 GPa, (h) $C2/m$ YbH₆ at 100 GPa, (i) $R\bar{3}$ -YbH₁₂ at 100 GPa.

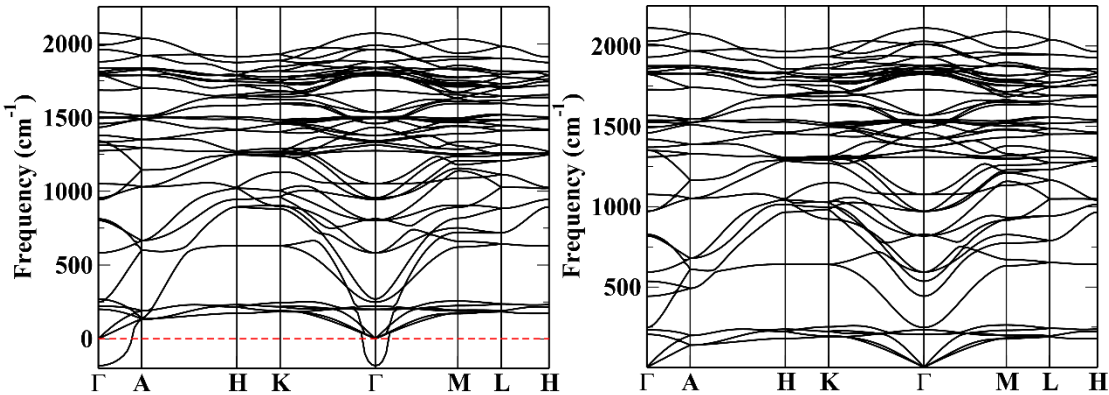


Fig. S5. Phonon dispersion of $P6_3/mmc$ -YbH₈ at 220 GPa (left) and 240 GPa (right).

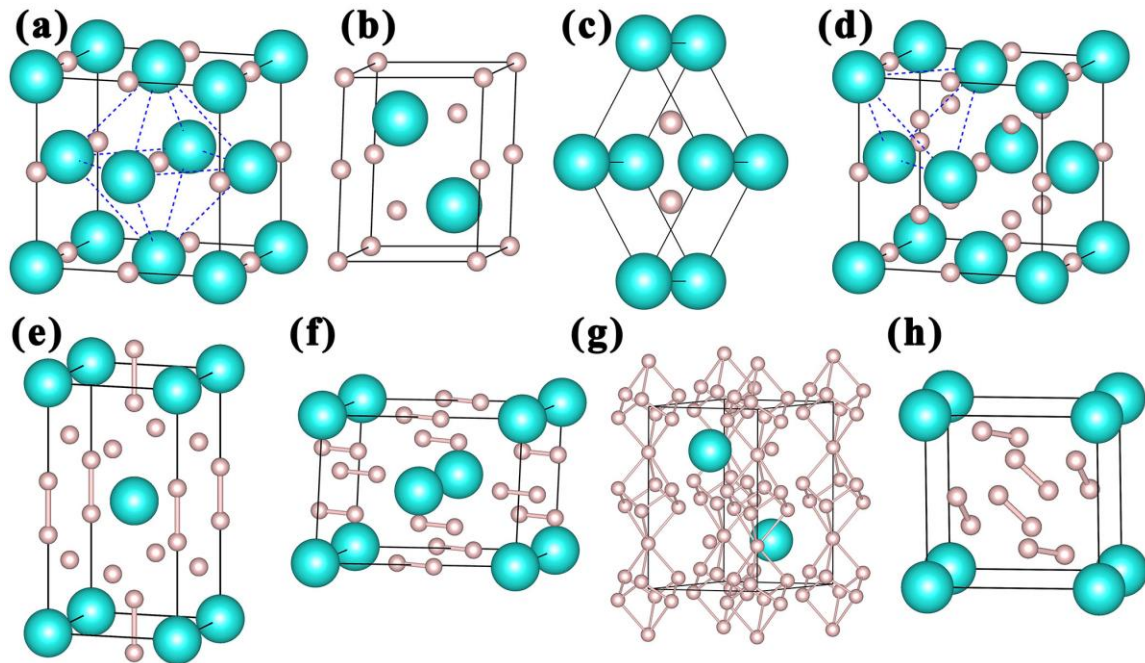


Fig. S6. The crystal structures of ytterbium hydrides (a) $Fm\bar{3}m$ -YbH, (b) $P6_3/mmc$ -YbH₂, (c) $P6/mmm$ -YbH₂, (d) $Fm\bar{3}m$ -YbH₃, (e) $I4/mmm$ -YbH₄, (f) $C2/m$ -YbH₆, (g) $P6_3/mmc$ -YbH₈, (h) $R\bar{3}$ -YbH₁₂.

Table S1. Calculated structural parameters of stable and metastable YbH_n (n=1-12) compounds.

Space group	Lattice parameters (Å)	Atoms	Atomic coordinates (fractional)			
			X	Y	Z	
YbH (100 GPa)	<i>Fm</i> $\bar{3}m$	$a=b=c=4.01$ $\alpha=\beta=\gamma=90^\circ$	H(4b) Yb(4a)	0.50 0.00	0.50 0.00	0.50 0.00
YbH (200 GPa)	<i>Cmcm</i>	$a=3.74$ $b=3.88$ $c=3.57$ $\alpha=\beta=\gamma=90^\circ$	H(4c) Yb(4c)	0.50 0.50	0.33 0.20	0.25 0.75
YbH ₂ (100 GPa)	<i>P</i> 6 ₃ /mmc	$a=b=3.22$ $c=4.10$ $\alpha=\beta=\gamma=90^\circ$	H(2d) H(2a) Yb(2c)	1/3 0.00 2/3	2/3 0.00 1/3	0.75 0.00 0.75
YbH ₂ (300 GPa)	<i>P</i> 6/mmm	$a=b=2.52$ $c=2.33$ $\alpha=\beta=90^\circ$ $\gamma=120^\circ$	H(2d) Yb(1a)	2/3 0.00	1/3 0.00	0.50 0.00
YbH ₃ (100 GPa)	<i>Fm</i> $\bar{3}m$	$a=b=c=4.36$ $\alpha=\beta=\gamma=90^\circ$	H(8c) H(4b) Yb(4a)	0.25 0.50 0.00	0.25 0.50 0.00	0.25 0.50 0.00
YbH ₄ (120 GPa)	<i>I</i> 4/mmm	$a=b=2.84$ $c=5.12$ $\alpha=\beta=\gamma=90^\circ$	H(4d) H(4e) Yb(2a)	0.50 0.50 0.00	0.00 0.50 0.00	0.25 0.094 0.00
YbH ₆ (100 GPa)	<i>C</i> 2/m	$a=5.14$ $b=3.80$ $c=3.04$ $\alpha=\gamma=90^\circ \beta=119^\circ$	H(8j) H(4i) Yb(2a)	0.11 0.61 0.00	-0.29 0.00 0.00	0.59 0.09 0.00
YbH ₆ (70 GPa)	<i>Im</i> $\bar{3}m$	$a=b=c=3.79$ $\alpha=\beta=\gamma=90^\circ$	H(12d) Yb(2a)	0.25 0.00	0.00 0.00	0.50 0.00
YbH ₆ (200 GPa)	<i>Im</i> $\bar{3}m$	$a=b=c=3.47$ $\alpha=\beta=\gamma=90^\circ$	H(12d) Yb(2a)	0.25 0.00	0.00 0.00	0.50 0.00
YH ₆ ^[17] (200 GPa)	<i>Im</i> $\bar{3}m$	$a=b=c=3.53$ $\alpha=\beta=\gamma=90^\circ$	H(12d) Yb(2a)	0.25 0.00	0.00 0.00	0.50 0.00
CaH ₆ ^[18] (150 GPa)	<i>Im</i> $\bar{3}m$	$a=b=c=3.50$ $\alpha=\beta=\gamma=90^\circ$	H(12d) Yb(2a)	0.25 0.00	0.00 0.00	0.50 0.00

YbH ₈ (300 GPa)	<i>P6₃/mmc</i>	<i>a</i> = <i>b</i> =3.10	H(12k)	0.16	0.33	0.94
		<i>c</i> =5.07	H(2d)	2/3	1/3	0.25
		$\alpha=\beta=90^\circ$	H(2b)	0.00	0.00	0.25
		$\gamma=120^\circ$	Yb(2c)	2/3	1/3	0.75
YbH ₁₂ (200 GPa)	<i>R</i> $\bar{3}$	<i>a</i> = <i>b</i> =4.44	H(18f)	0.24	0.25	-0.56
		<i>c</i> =5.52	H(18f)	-0.17	-0.71	0.03
		$\alpha=\beta=90^\circ$	Yb(3a)	0.00	0.00	0.00
		$\gamma=120^\circ$				

5. Electronic properties of YbH₆

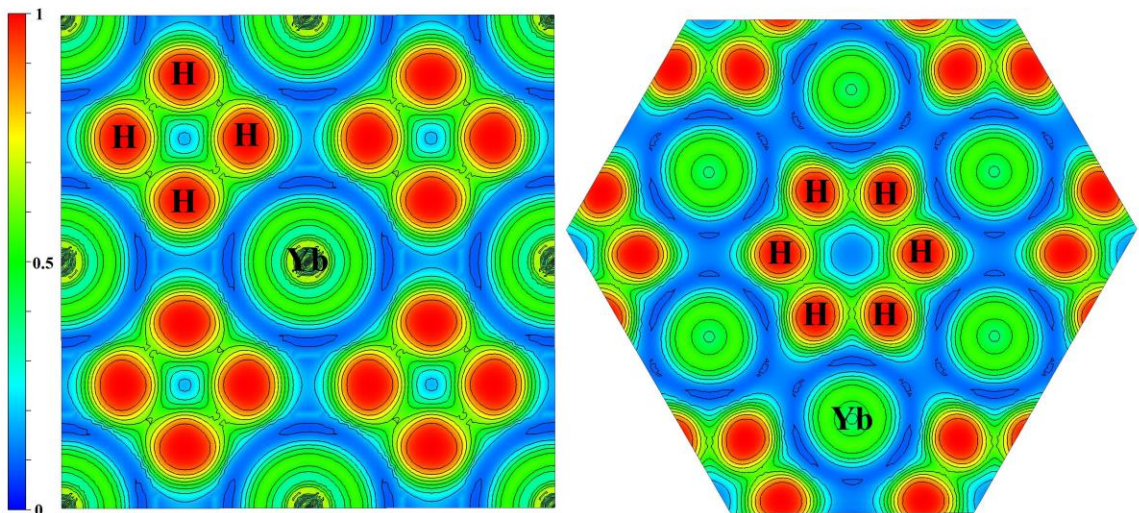


Fig. S7. The electron localization functions (ELF) of cubic YbH₆ at 70 GPa for [0 0 1] plane (left panel) and [1 1 -1] plane (right panel). The isopleth curves are plotted with interval 0.1.

6. Convex hull diagram of Lu-H and Tm-H

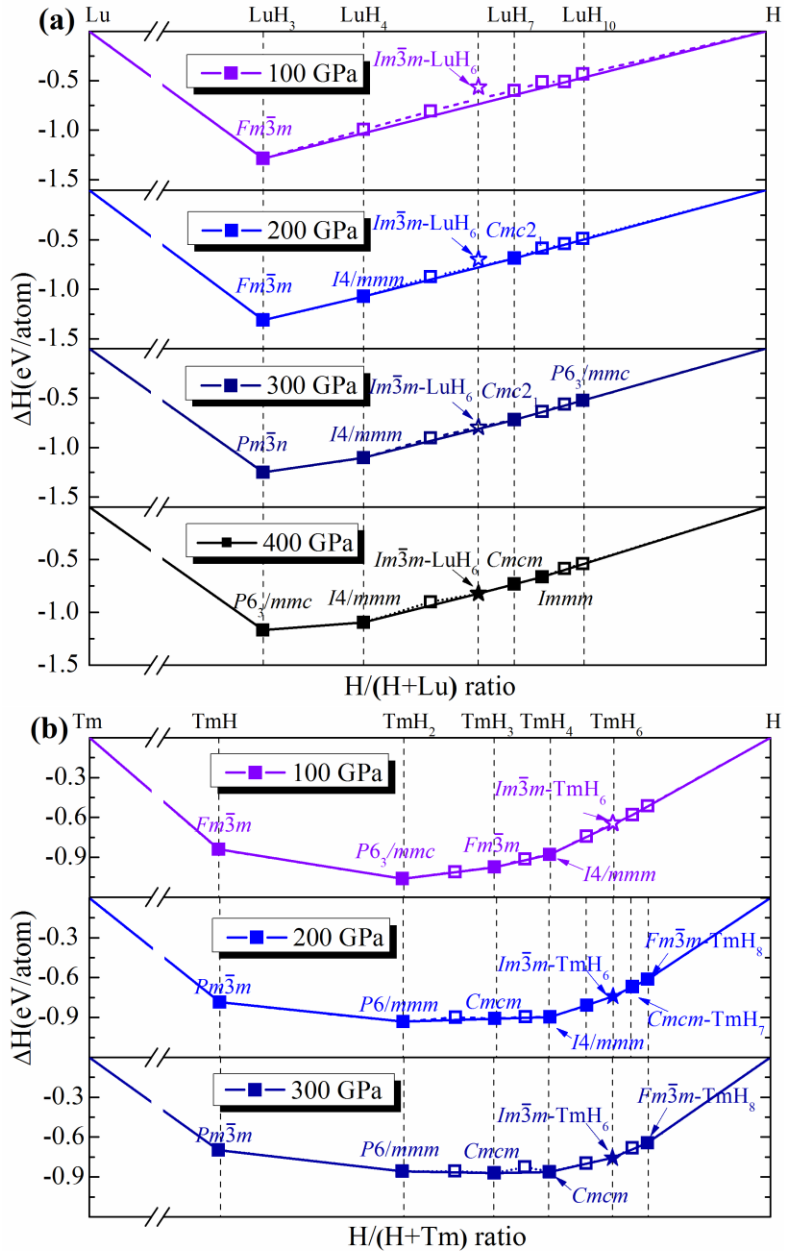


Fig. S8. Convex hull of (a) Lu-H at 100, 200, 300, and 400 GPa, (b) Tm-H at 100, 200 and 300 GPa. The solid and open symbols indicate that the structures are thermodynamic stable and unstable, respectively. The open stars indicate the cubic LuH₆ (10 meV above the convex hull at 300 GPa) and TmH₆ (8 meV above the convex hull at 100 GPa).

Table S2. Calculated structural parameters of Lu-H and Tm-H compounds.

Space group	Lattice parameters (Å)	Atoms	Atomic coordinates (fractional)			
			X	Y	Z	
LuH ₃ (100 GPa)	<i>Fm</i> $\bar{3}m$	$a=b=c=4.35$ $\alpha=\beta=\gamma=90^\circ$	H(8c) H(4b) Lu(4a)	0.25 0.50 0.00	0.25 0.50 0.00	0.25 0.50 0.00
LuH ₄ (100 GPa)	<i>I</i> 4/ <i>mmm</i>	$a=b=3.56$ $c=3.13$ $\alpha=\beta=\gamma=90^\circ$	H(8j) Lu(2a)	0.20 0.00	0.50 0.00	0.00 0.00
LuH ₅ (200 GPa)	<i>P</i> 4/ <i>nmm</i>	$a=b=3.43$ $c=3.55$ $\alpha=\beta=\gamma=90^\circ$	H(2b) H(8i) Lu(2c)	0.50 0.50 0.00	0.50 0.74 0.50	0.50 0.80 0.74
LuH ₆ (100 GPa)	<i>Fm</i> $\bar{3}m$	$a=b=c=3.69$ $\alpha=\beta=\gamma=90^\circ$	H(8c) H(4b) Lu(4a)	0.25 0.50 0.00	0.25 0.50 0.00	0.25 0.50 0.00
LuH ₇ (150 GPa)	<i>Cmc</i> 2 ₁	$a=3.27$ $b=5.50$ $c=5.60$ $\alpha=\beta=\gamma=90^\circ$	H(8b) H(8b) H(4a) H(4a) H(4a) Lu(4a)	0.74 0.71 0.50 0.50 0.50 0.50	0.09 0.04 0.19 0.99 0.68 0.33	0.14 0.72 0.63 0.93 0.85 0.93
TmH (50 GPa)	<i>Fm</i> $\bar{3}m$	$a=b=c=4.24$ $\alpha=\beta=\gamma=90^\circ$	H(4b) Tm(4a)	0.50 0.00	0.50 0.00	0.50 0.00
TmH ₂ (50 GPa)	<i>P</i> 6 ₃ / <i>mmc</i>	$a=b=2.39$ $c=4.39$ $\alpha=\beta=\gamma=90^\circ$	H(2d) H(2a) Tm(2c)	1/3 0.00 2/3	2/3 0.00 1/3	0.75 0.00 0.75
TmH ₃ (50 GPa)	<i>Fm</i> $\bar{3}m$	$a=b=c=4.58$ $\alpha=\beta=\gamma=90^\circ$	H(8c) H(4b) Tm(4a)	0.25 0.50 0.00	0.25 0.50 0.00	0.25 0.50 0.00
TmH ₄ (50 GPa)	<i>I</i> 4/ <i>mmm</i>	$a=b=3.08$ $c=5.40$ $\alpha=\beta=\gamma=90^\circ$	H(4d) H(4e) Tm(2a)	0.50 0.50 0.00	0.00 0.50 0.00	0.25 0.094 0.00
TmH ₆ (50 GPa)	<i>Fm</i> $\bar{3}m$	$a=b=c=3.85$ $\alpha=\beta=\gamma=90^\circ$	H(8c) H(4b) Tm(4a)	0.25 0.50 0.00	0.25 0.50 0.00	0.25 0.50 0.00

7. Equations for calculating T_c and related parameters

(1) Self-consistent iteration solution of the Eliashberg equation

The Eliashberg equation has a form^[10,19,20]:

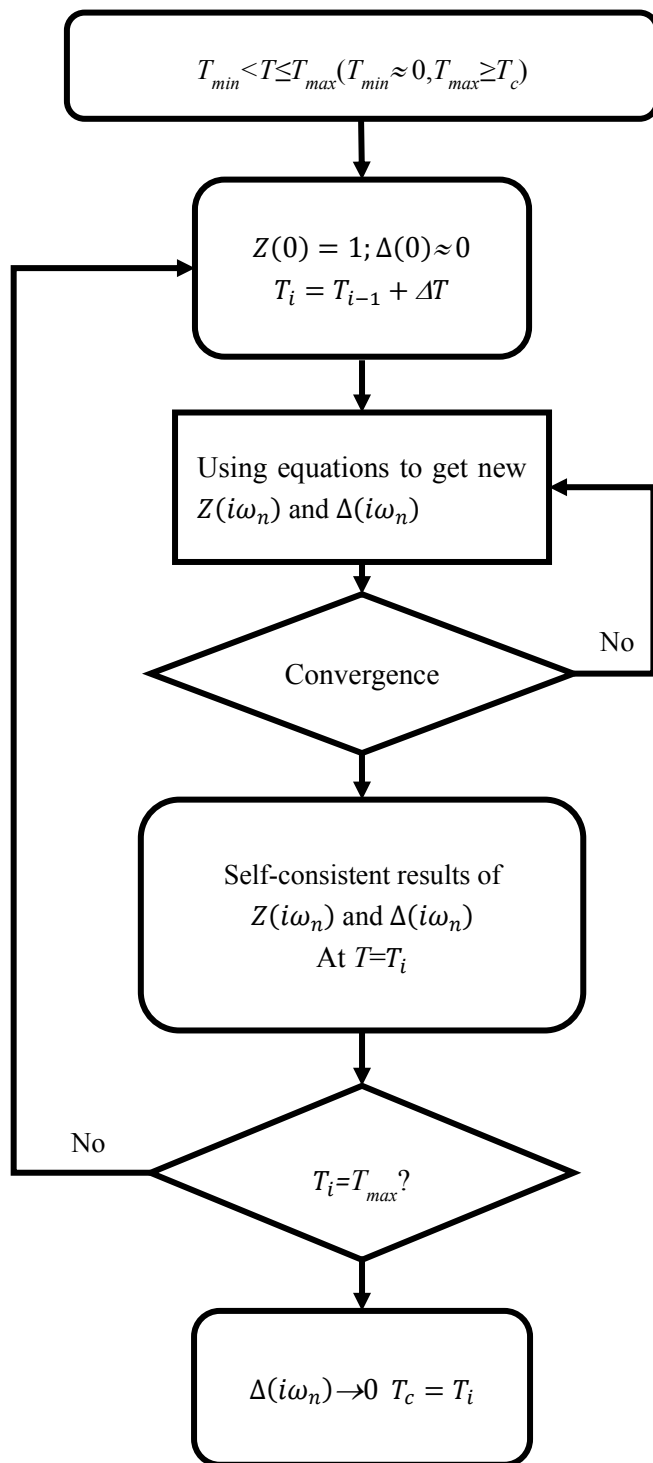
$$\Delta(i\omega_n)Z(i\omega_n) = \frac{\pi T}{N_F} \sum_{n'} \frac{\Delta(i\omega'_n)}{\sqrt{\omega'^2_n + \Delta^2(i\omega'_n)}} \times [\lambda(\omega_n - \omega_{n'}) - N_F \mu^*] \delta(\epsilon) \quad (\text{S1})$$

$$Z(i\omega_n) = 1 + \frac{\pi T}{N_F \omega_n} \sum_{n'} \frac{\omega'_n}{\sqrt{\omega'^2_n + \Delta^2(i\omega'_n)}} \lambda(\omega_n - \omega_{n'}) \delta(\epsilon) \quad (\text{S2})$$

Here functions $\Delta(i\omega_n)$ and $Z(i\omega_n)$ represent pairing order parameter and the renormalization function, N_F is the density of electronic states at the Fermi level, and $\delta(\epsilon)$ is the Dirac delta function. $i\omega_n = i(2n + 1)\pi T_c$ are the fermion Matsubara frequencies (we employ the thermodynamic Green's functions formalism (see,e.g.,^[21]); μ^* is the Coulomb pseudopotential, for which we use the widely accepted range of 0.1-0.13. $\lambda(\omega_n - \omega_{n'})$ contains the electron-phonon coupling matrix, phonon propagator. and the phonon density of states, and is given by:

$$\lambda(\omega_n - \omega_{n'}) = \int_0^\infty d\omega \frac{2\omega}{(\omega_n - \omega_{n'})^2 + \omega^2} \alpha^2 F(\omega) \quad (\text{S3})$$

The equations for the order parameter and the renormalization function form a coupled nonlinear system and are solved self-consistently. We evaluated the renormalization function and the order parameter for each Matsubara frequency along the imaginary energy axis. After calculating $Z(i\omega_n)$ and $\Delta(i\omega_n)$, an analytic continuation is performed to the real axis using the Pade' functions. The calculation is performed for each T ($T_{\min} < T \leq T_{\max}$) ($T_{\min} \approx 0$ and $T_{\max} \geq T_c$). The critical temperature T_c is obtained as an asymptotic value as $\Delta(i\omega_n)$ tends to zero.



(2) The McMillan–Allen–Dynes equation

The McMillan–Allen–Dynes equation (Mc-A-D) is the approximate analytic solution of the Eliashberg equations at $\lambda < 1.5$; it has a form [11]:

$$T_c = \frac{\omega_{log}}{1.2} \exp \left[-\frac{1.04(1+\lambda)}{\lambda - \mu^*(1+0.62\lambda)} \right], \quad (\text{S4})$$

If $\lambda > 1.5$, one should use the more general equation containing the corrections f_1 and f_2 :

$$T_c = \frac{f_1 f_2 \omega_{log}}{1.2} \exp \left[-\frac{1.04(1+\lambda)}{\lambda - \mu^*(1+0.62\lambda)} \right], \quad (\text{S5})$$

where f_1 and f_2 are given by [11]:

$$f_1 = \sqrt[3]{1 + \left(\frac{\lambda}{2.46(1+3.8\mu^*)} \right)^{\frac{3}{2}}}, \quad f_2 = 1 + \frac{\left(\frac{\bar{\omega}_2}{\omega_{log}} - 1 \right) \lambda^2}{\lambda^2 + [1.82(1+6.3\mu^*) \frac{\bar{\omega}_2}{\omega_{log}}]^2}, \quad (\text{S6})$$

Here $\bar{\omega}_2$ is the mean square frequency,

$$\bar{\omega}_2 = \sqrt{\frac{2}{\lambda} \int \alpha^2 F(\omega) \omega d\omega}, \quad (\text{S7})$$

ω_{log} is the logarithmic average frequency. The ω_{log} and EPC constant λ are defined by the relations:

$$\omega_{log} = \exp \left[\frac{2}{\lambda} \int \frac{d\omega}{\omega} \alpha^2 F(\omega) \ln \omega \right], \quad (\text{S8})$$

$$\lambda = 2 \int \frac{\alpha^2 F(\omega)}{\omega} d\omega, \quad (\text{S9})$$

(3) Gor'kov-Kresin equation

Gor'kov and Kresin (G-K) introduced the coupling constants λ_{opt} and λ_{ac} describing the interaction of electrons with optical and acoustic phonons^[14,22]. The generalized Eliashberg equation has the form (at $T=T_c$):

$$\Delta(\omega_n)Z = \pi T \sum_{\omega_{n'}} \left[\lambda_{opt} \frac{\tilde{\Omega}_{opt}^2}{\tilde{\Omega}_{opt}^2 + (\omega_n - \omega_{n'})^2} + \lambda_{ac} \frac{\tilde{\Omega}_{ac}^2}{\tilde{\Omega}_{ac}^2 + (\omega_n - \omega_{n'})^2} \right] \frac{\Delta(\omega_{n'})}{|\omega_{n'}|} \Big|_{T=T_c}, \quad (\text{S10})$$

$$\lambda_{ac} = 2 \int_0^{\Omega_1} \frac{\alpha^2 F(\omega)}{\omega} d\omega, \quad \lambda_{opt} = 2 \int_{\Omega_1}^{\Omega_m} \frac{\alpha^2 F(\omega)}{\omega} d\omega, \quad \lambda_{ac} + \lambda_{opt} = \lambda, \quad (\text{S11})$$

where ω_1 is the maximum frequency for the acoustic modes, ω_m is the maximum frequency's value. The mean square average frequency values are defined as follows:

$$\tilde{\omega}_{\text{ac}} = \langle \omega_{\text{ac}}^2 \rangle^{\frac{1}{2}}, \langle \omega_{\text{ac}}^2 \rangle = \frac{2}{\lambda_{\text{ac}}} \int_0^{\omega_1} d\omega \cdot \omega^2 \frac{\alpha^2 F(\omega)}{\omega} = \frac{2}{\lambda_{\text{ac}}} \int_0^{\omega_1} \alpha^2 F(\omega) \omega d\omega, \quad (\text{S12})$$

$$\tilde{\omega}_{\text{opt}} = \langle \omega_{\text{opt}}^2 \rangle^{\frac{1}{2}}, \langle \omega_{\text{opt}}^2 \rangle = \frac{2}{\lambda_{\text{opt}}} \int_{\omega_1}^{\omega_m} d\omega \cdot \omega^2 \frac{\alpha^2 F(\omega)}{\omega} = \frac{2}{\lambda_{\text{opt}}} \int_{\omega_1}^{\omega_m} \alpha^2 F(\omega) \omega d\omega, \quad (\text{S13})$$

For our predicted hydrides the $\lambda_{\text{ac}} \ll \lambda_{\text{opt}}$, we assume that:

$$T_c = T_c^{\text{opt}} + \Delta T_c^{\text{ac}}, \text{ and } T_c^{\text{opt}} \gg \Delta T_c^{\text{ac}} \quad (\text{S14})$$

As a result, the expression for T_c can be written in the form:

$$T_c = \left[1 + 2 \frac{\lambda_{\text{ac}}}{\lambda_{\text{opt}} - \mu^*} \cdot \frac{1}{1 + \rho^{-2}} \right] T_c^0, \rho = \frac{\tilde{\omega}_{\text{ac}}}{\pi T_c^0}, T_c^0 \equiv T_c^{\text{opt}}. \quad (\text{S15})$$

Here the T_c^0 is defined as the transition temperatures caused by the interaction of electrons with optical phonons only; for $\lambda_{\text{opt}} \leq 1.5$:

$$T_c^0 = \frac{\tilde{\omega}_{\text{opt}}}{1.2} \exp \left[-\frac{1.04(1+\lambda_{\text{opt}})}{\lambda_{\text{opt}} - \mu^*(1+0.62\lambda_{\text{opt}})} \right]. \quad (\text{S16})$$

For $\lambda_{\text{opt}} > 1.5$:

$$T_c^0 = \frac{0.25\tilde{\omega}_{\text{opt}}}{[e^{\tilde{\lambda}_{\text{eff}}} - 1]^{1/2}}. \quad (\text{S17})$$

Here the λ_{eff} is defined as follows:

$$\lambda_{\text{eff}} = (\lambda_{\text{opt}} - \mu^*) [1 + 2\mu^* + \lambda_{\text{opt}}\mu^* t(\lambda_{\text{opt}})]^{-1}, \quad (\text{S18})$$

$$t(x) = 1.5 \exp(-0.28x). \quad (\text{S19})$$

The following expression:

$$\alpha = \frac{1}{2} [1 - 4 \frac{\lambda_{\text{ac}}}{\lambda_{\text{opt}}} \frac{\rho^2}{(\rho^2 + 1)^2}] \quad (\text{S20})$$

allows us to calculate the isotope coefficient α .

8. Superconductive properties

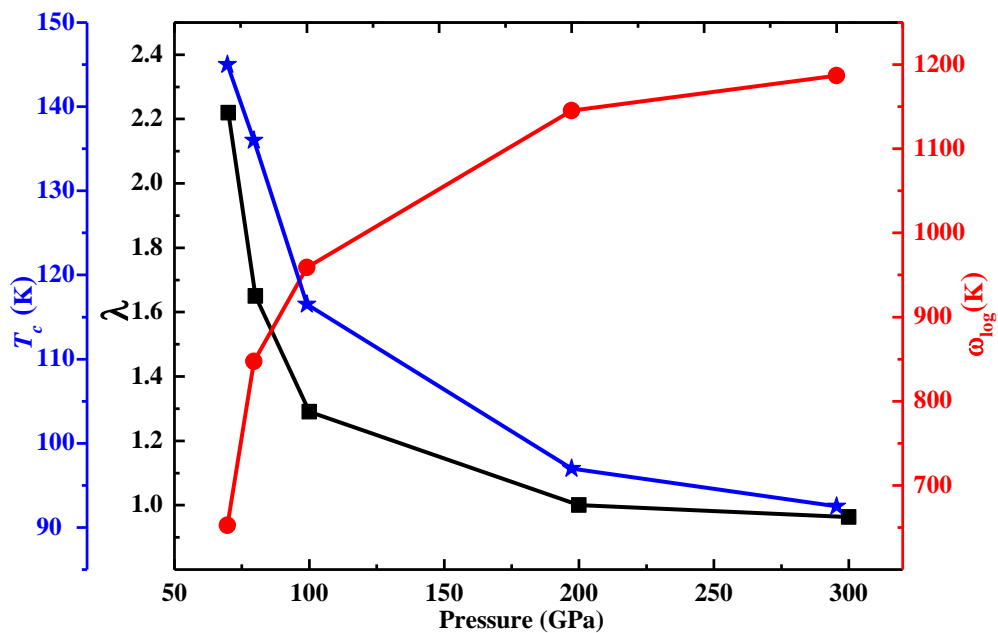


Fig. S9. The EPC parameter λ , logarithmic average frequency ω_{\log} , and T_c of YbH₆ versus pressures.

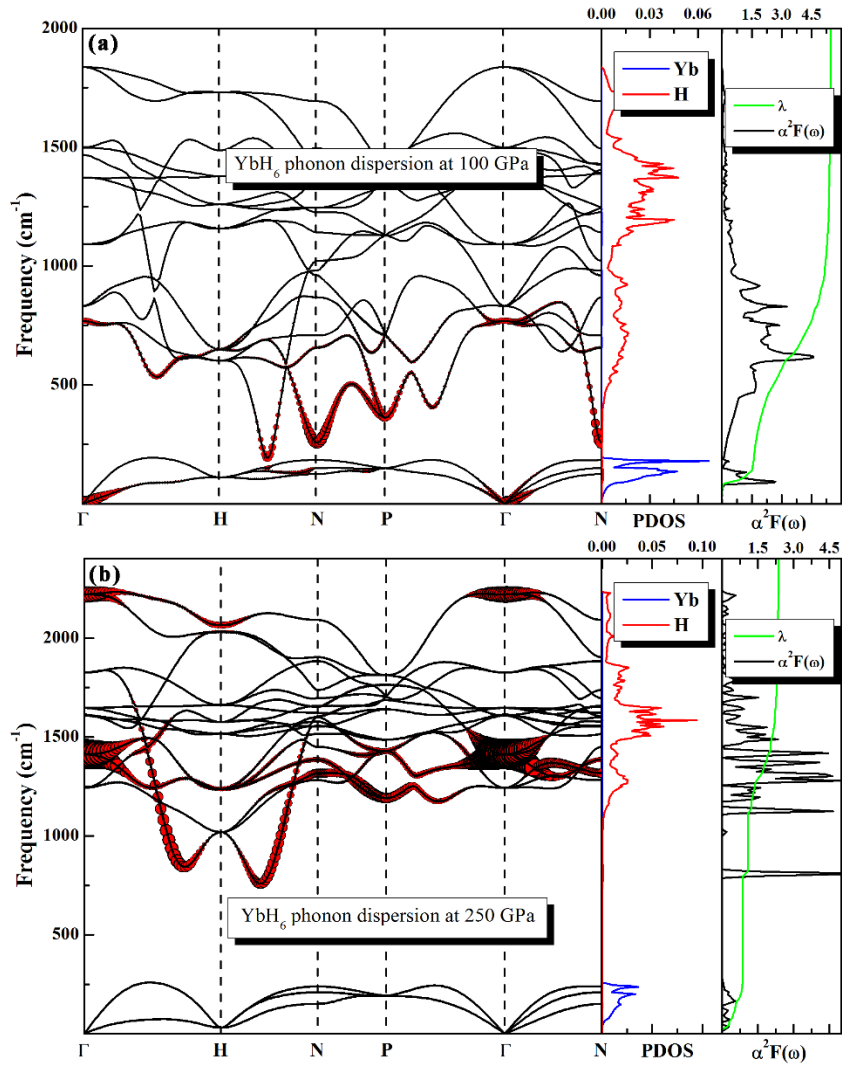


Fig. S10. Phonon dispersion, phonon density of state, spectral function ($\alpha^2 F(\omega)$) and integral EPC λ of $Im\bar{3}m$ -YbH₆ with frozen-*f* electrons at 100 GPa (a) and 250 GPa (b). Red circles with radius proportional to the EPC strength.

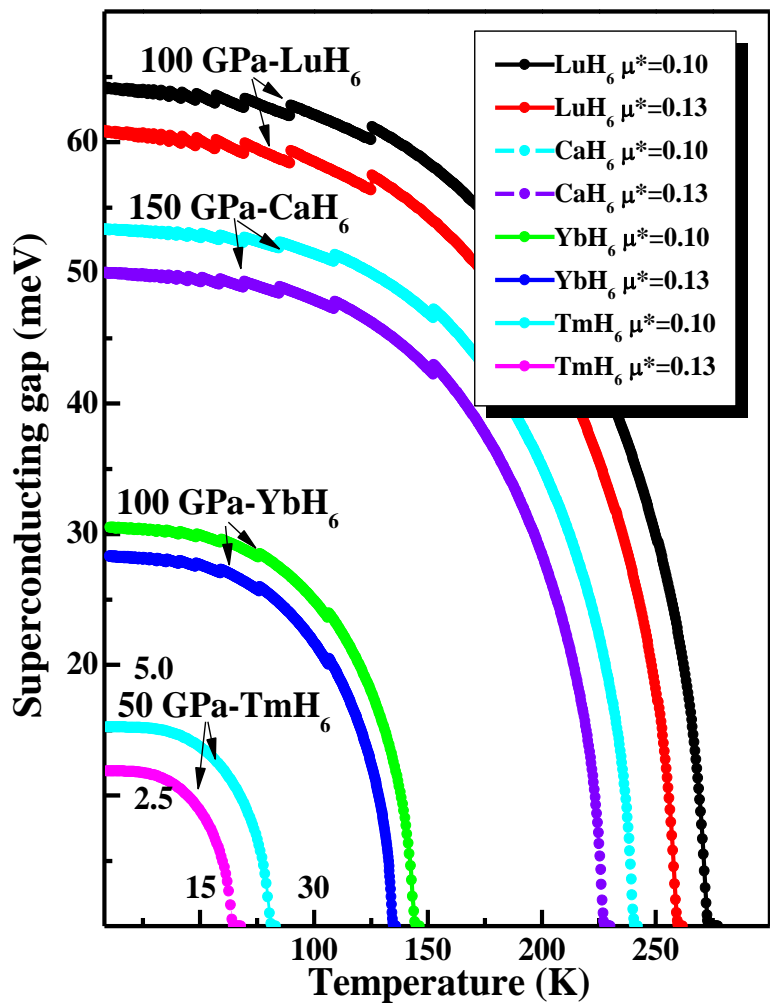


Fig. S11. The superconducting gap for XH₆ (X=Ca, Tm, Yb, Lu) at different pressure.

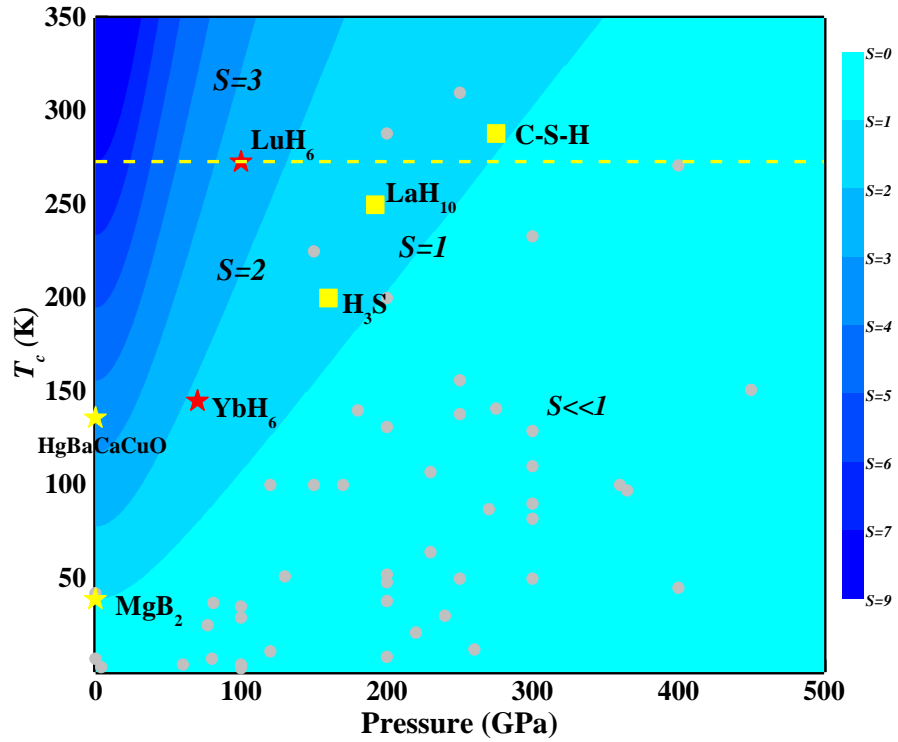


Fig. S12. The superconducting critical temperature T_c as a function of the pressure for different hydrides. Small circles correspond to predictions as summarized in table 1 in [23]. Yellow stars represent $S(\text{MgB}_2) = 1$ and $S(\text{HgBaCaCuO}) = 3.5$, red stars represent $S(\text{LuH}_6) = 2.5$ and $S(\text{YbH}_6) = 1.8$ and yellow square represent $S(\text{C-S-H}) = 1.1$, $S(\text{H}_3\text{S}) = 1.3$ and $S(\text{LaH}_{10}) = 1.3$ [24]. The yellow dash-line represent ice point temperature. The colored contours correspond to the figure of merit $S = \frac{T_c}{\sqrt{T_{c,\text{MgB}_2}^2 + P^2}}$, ($T_{c,\text{MgB}_2} = 39$ K)

Table S3. The calculated EPC parameter λ , logarithmic average phonon frequency ω_{log} (K), electronic density of states at Fermi level $N(\epsilon_f)$ (states/spin/Ry/f.u.), isotope coefficients α and superconducting transition temperatures T_c (K) with $\mu^*=0.1-0.13$ at corresponding pressures P (GPa).

Structure	P	λ	ω_{log}	$N(\epsilon_f)$	α	T_c (K) ^a	Mc-A-D T_c (K) ^b	AI T_c (K)	G-K T_c (K)
<i>Im</i> $\bar{3}m$ YbH ₆	70	2.22	652.4	8.4	0.48	90-94	114-125	125-145	121-131
	100	1.29	959.0	7.6	0.44	83-93	87-101	99-116	98-102
	200	1.00	1146.5	6.8	0.38	69-80	72-85	82-96	78-91
	300	0.96	1186.9	6.4	0.35	65-77	69-80	77-92	72-87
<i>Im</i> $\bar{3}m$ LuH ₆	100	3.60	750.5	4.8	0.49	140-146	204-222	260-273	227-243
	200	1.77	1366.2	4.2	0.47	166-180	190-209	231-250	190-210
<i>Im</i> $\bar{3}m$ TmH ₆	50	0.72	611.9	29.6	0.47	17-22	18-23	19-24	19-25
<i>Im</i> $\bar{3}m$ EuH ₆	160	0.13	511.1	64.4	\	0	0	0	0
<i>Im</i> $\bar{3}m$ CaH ₆	150	2.67	1027.1	2.4	0.38	165-175	205-222	227-241	220-236
<i>Im</i> $\bar{3}m$ YH ₆	120	3.06	829.0	4.7	0.46	143-150	195-213	244-257	218-234
<i>Im</i> $\bar{3}m$ H ₃ S	200	1.88	1266.0	3.1	0.35	162-175	186-204	212-223	206-229

^a T_c was estimated using Allen-Dynes- McMillian equation with $f_1f_2 = 1$ (Eq. S1).

^b T_c was estimated using Allen-Dynes- McMillian equation with $f_1f_2 \neq 1$ (Eq. S2).

Table S4. The calculated EPC parameter λ , logarithmic average phonon frequency ω_{log} (K), electronic density of states at Fermi level $N(\varepsilon_f)$ (states/spin/Ry/f.u.) and superconducting transition temperatures T_c (K) of LuH_n (n=3,4,5,7) with $\mu^*=0.1-0.13$ at corresponding pressures P (GPa).

Structure	P (GPa)	λ	ω_{log} (K)	$N(\varepsilon_f)$	T_c (K) ^a
<i>Fm</i> $\bar{3}m$ LuH ₃	100	0.4	670	2.0	1-3
<i>I4/mmm</i> LuH ₄	100	1.5	632	3.4	65-71
<i>P4/nmm</i> LuH ₅	150	1.7	703	6.8	82-89
<i>Cmc2</i> ₁ LuH ₇	150	0.6	1060	3.9	26-34

^a T_c was estimated using Allen-Dynes- McMillian equation with $f_1f_2 = 1$ (Eq. S1).

Table S5. The calculated T_c of XD₆ (X=Yb, Lu, Y, Ca, and Sc) at different pressures.

Parameter	YbD ₆	LuD ₆	YD ₆	CaD ₆	ScD ₆
	70 GPa	100 GPa	120 GPa	150 GPa	300 GPa
T_c^D (K)	87-94	162-173	158-170	169-181	136-152

References

- [1] Pickard C J and Needs R J 2011. *J Phys Condens Matter* **23** 053201
- [2] Pickard C J and Needs R J 2006. *Phys. Rev. Lett.* **97** 045504
- [3] Segall M D, Lindan P J D, Probert M J, Pickard C J, Hasnip P J, Clark S J and Payne M C 2002. *J Phys Condens Matter* **14** 2717
- [4] Payne M C, Teter M P, Allan D C, Arias T A and Joannopoulos J D 1992. *Rev. Mod. Phys.* **64** 1045
- [5] Clark S J, Segall M D, Pickard C J, Hasnip P J, Probert M J, Refson K and Payne M C 2005. *Z. Kristallogr.* **220** 567
- [6] Vanderbilt D 1990. *Phys. Rev. B* **41** 7892
- [7] Perdew J P, Burke K and Ernzerhof M 1996. *Phys. Rev. Lett.* **77** 3865
- [8] Monkhorst H J and Pack J D 1976. *Phys. Rev. B* **13** 5188
- [9] Giannozzi P, Baroni S, Bonini N, Calandra M, Car R, Cavazzoni C, Ceresoli D, Chiarotti G L, Cococcioni M, Dabo I *et al.* 2009. *Journal of Physics Condensed Matter* **21**
- [10] Eliashberg G M 1960. *J. Exp. Theor. Phys.* **11** 696
- [11] Allen P B and Dynes R C 1975. *Phys. Rev. B* **12** 905
- [12] Bergmann G and Rainer D 1973. *Zeitschrift für Physik* **263** 59
- [13] Rainer D and Bergmann G 1974. *J. Low Temp. Phys.* **14** 501
- [14] Gor'kov L P and Kresin V Z 2018. *Rev. Mod. Phys.* **90** 16
- [15] Klotz S, Casula M, Komatsu K, Machida S and Hattori T 2019. *Phys. Rev. B* **100** 5
- [16] Olsen J S, Buras B, Gerward L, Johansson B, Lebech B, Skriver H L and Steenstrup S 1984. *Phys. Scr.* **29** 503
- [17] Peng F, Sun Y, Pickard C J, Needs R J, Wu Q and Ma Y M 2017. *Phys. Rev. Lett.* **119** 6
- [18] Wang H, John S T, Tanaka K, Iitaka T and Ma Y 2012. *Proc. Natl. Acad. Sci. U. S. A.* **109** 6463
- [19] McMillan W L 1968. *Physical Review* **167** 331
- [20] Dynes R C 1972. *Solid State Commun.* **10** 615
- [21] Abrikosov A A, Gorkov L P and Dzyaloshinski I E, *Methods of quantum field theory in statistical physics* (Courier Corporation, 2012).
- [22] Gor'kov L P and Kresin V Z 2016. *Sci. Rep.* **6** 25608
- [23] Bi T, Zarifi N, Terpstra T and Zurek E 2019. *Reference Module in Chemistry, Molecular Sciences and Chemical Engineering*
- [24] Pickard C J, Errea I and Eremets M I 2020. *Annu Rev Condens Matter Phys* **11** 57